

Study of Porosity and Surface Groups of Activated Carbons Produced from Alternative and Renewable Biomass: Buriti Petiole

Cristiane Freitas de Almeida^a, Robson Carlos de Andrade^a, Giulyane Felix de Oliveira^a, Patrícia Hatsue Suegama^a, Eduardo José de Arruda^a, José Augusto Texeira^b, Cláudio Teodoro de Carvalho^{a,*}

^aUniversidade Federal da Grande Dourados, Rodovia Dourados - Itahum, Km 12. Cidade Universitária, Dourados-MS, 79804-970, Brazil.

^bInstituto de Química, UNESP – Universidade Estadual Paulista Julio de Mesquita, Araraquara-SP, 14801-970, Brazil.

Article history: Received: 11 July 2016; accepted: 31 January 2017. Available online: 05 March 2017. DOI: <http://dx.doi.org/10.17807/orbital.v9i1.878>

Abstract: This study reports the production of activated carbon (AC) from chemical activation with sodium hydroxide in pyrolysis temperature of 500 to 600 °C using alternative and renewable material, Buriti petiole. The characterization of the material was performed by simultaneous thermogravimetry-differential thermal analysis (TG-DTA), scanning electron microscopy (SEM), nitrogen adsorption-desorption isotherms at -196 °C by the BET (Brunauer, Emmett and Teller) and BJH (Barrett, Joyner and Halenda) methods for mesoporous materials. Infrared spectroscopy (FT-IR) and TG/DTG-FTIR coupled system were used to study the surface groups. Adsorption tests for the activated carbons samples (ACs) were carried out using the methylene blue (MB) cationic and anionic orange G (OG) dyes, the most satisfactory results were methylene blue dye. These results indicated the formation of mesoporous adsorbent materials with BET surface areas obtained between 340 m²g⁻¹ and 1715 m²g⁻¹. The chemical activation of the carbons with sodium hydroxide produced highly mesoporous material suitable for adsorption of cationic and anionic dyes in aqueous solution.

Keywords: buriti petiole; activated carbon; FT-IR; TG/DTG/FT-IR; SEM; BET

1. INTRODUCTION

As industrial waste has increased worldwide driven by industrialization effort, it has also grown the search for technologies which can minimize the environmental impact caused by toxic or hazardous substances from this waste, addressing many existing national environmental regulations. Within this range of technologies, activated carbons from alternative sources of renewable raw materials have played an important role [1-4].

Activated carbons (AC) are adsorbents widely used for this purpose, since they present high removal capacity, adsorbent regeneration and can be easily applied to various industrial processes such as purification and deodorization due to their high porosity and surface area, as well as to the presence of functional groups [5-10]. AC can be produced from lignocellulosic materials like pine woods, eucalyptus, coconut husk, rice husk, fruit seeds, turf, among others,

due to their high concentration of carbon, an essential component for the production of AC of high quality. Although agribusiness waste has provided most of the raw material (RM) for the AC production sector, alternative renewable materials obtained at low cost directly from nature can be a promising option, not only due to their already proven suitability as excellent precursor materials but also due to their potential to generate economic, social and environmental benefits driven by the obtainment of high added value products [11-15].

In this study, the lignocellulosic material used for the activated carbon samples (ACs) production was the petiole of the Buriti palm (*Mauritia flexuosa* L.f), a palm that grows in wet areas in South America and is widely found in areas of the Amazon rainforest and Brazilian Cerrado [16-17]. The ACs were prepared by chemical activation process with sodium hydroxide. The material characterized showed excellent porosity increase in the mesopores region and adequate surface

*Corresponding author. E-mail: claudioteodor@gmail.com

area to the adsorption of organic and inorganic molecules found in industrial wastes [1–15].

2. MATERIAL AND METHODS

2.1. Production of the activated carbons

The RM Buriti petiole used in the AC production was collected from dead leaves of Buriti palm in a farm in the countryside of the city of Coxim, state of Mato Grosso do Sul, Brazil. The material raw underwent a process where the outer fibers of the petiole were removed, cut into small pieces and ground in a knife mill. The material was sieved to particle sizes of 0.30 mm using a sieve of 48 mesh.

The ACs were obtained by chemical activation method using sodium hydroxide (Merck, 99% purity) as activating agent. The RM was impregnated with sodium hydroxide solution in the ratios w/w 1:2:3 NaOH/RM. After impregnation, the RM was kept for 24 hours in an oven at 115 °C and then undergone pyrolysis in inert N₂ atmosphere with a flow rate of 20 mL min⁻¹, using a tubular furnace of stainless steel 20 cm long and 5 cm in diameter inserted in a muffle furnace [18–20]. The parameters utilized in the pyrolysis process are described in Table 1.

Table 1. Parameters used in the pyrolysis process for the ACs production.

Samples	Isotherms of activation / °C	Activation time / h	NaOH / RM ratios
AC1	500	3	1:1
AC2	500	3	2:1
AC3	500	3	3:1
AC4	600	3	1:1
AC5	600	3	2:1
AC6	600	3	3:1

AC = activated carbon, NaOH = activating agent, h = hours, RM = raw material

The ACs obtained were washed out with distilled water until neutral pH to remove the activating agent and unclog the pores formed.

2.2. Characterization of the activated carbons

Thermogravimetric analysis

Simultaneous TG–DTA and TG/DTG curves were obtained by using the thermal analysis equipment TA Instruments model SDT 2960, with weight

sensitivity of 0.1 µg, using air or N₂ (99 % pure) as purge gas with a flow rate of 100 mL min⁻¹. Heating rates of 20 °C min⁻¹ (air) and 10 °C (N₂) were adopted with sample masses of about 5.0 mg using alumina crucibles with heating rate between 30 and 1000 °C for the samples.

Surface study by TG/DTG/FT–IR coupled system and FT–IR

The gaseous products CO and CO₂ released between 30 – 1000 °C from the surface groups were monitored by a Mettler TG–DSC Thermogravimetric Analyzer coupled to a Nicolet FT–IR spectrophotometer with gas cell and DTGS KBr detector. The gas cell and the transfer line were kept heated at 250 °C and both purged with dry N₂ (50 mL min⁻¹). The FT–IR spectra were recorded with 32 scans per spectrum at 4 cm⁻¹ resolution.

The surface groups of the ACs were also studied by Fourier Transform-Infrared Spectroscopy (FT–IR) in solid state. The analysis of the ACs was carried out using a Jasco 4100 spectrophotometer in the spectral range of 700 to 4000 cm⁻¹, using attenuated total reflectance (ATR) with zinc selenide window. The AC samples were preheated at 110 °C for 12 hours to remove adsorbed water.

Scanning electron microscopy analysis

The morphology of the materials was studied using a scanning electron microscope (SEM), model Jeol JSM–6610LV, with accelerating voltage of 10.0 kV and focus distance between 9 and 10 mm. The magnification range used during the analysis ranged from 300x to 3000x. Before the analysis, the samples were fixed with carbon tape and coated with gold in a metallization process to obtain good surface conductivity.

Textural analysis

The textural properties of the carbons were analyzed by nitrogen adsorption at –196 °C using the Micromeritics ASAP 2020 Physisorption Analyzer, at a relative pressure range of 10⁻⁷ to 0.99 P/P₀. Before the analysis, all samples were degassed at 300 °C for 10h at 0.5 µm Hg vacuum. The specific surface area was measured by BET (Brunauer–Emmett–Teller) method using the adsorption data at the relative pressure range (P/P₀) of 0.05 to 0.3 and the pore

diameter distribution was obtained by applying the BJH method (Barret, Joyner and Halenda).

Adsorption tests

For the adsorption tests in liquid phase, 500 mg of each ACs were placed in contact with 100 mL of the solutions of the dyes MB and OG in a concentration of 100 mg L⁻¹, kept under stirring of 125 rpm for 4h at the temperature of 30 °C and had their pH adjusted to 7. Then, aliquots of the material were centrifuged and the remaining concentrations were monitored by UV–Visible (Cary 50) in the wavelengths of 472 nm for the MB and 665 nm for OG. The OG and MB dyes concentrations were calculated considering the calibration curves previously obtained with experiments done in triplicate.

3. RESULTS AND DISCUSSION

3.1. Pyrolysis study of the raw material by TG/DTG under inert N₂ atmosphere

The thermal analysis of the raw material (RM), Fig. 1, allowed to monitor the thermal decomposition range of the material and determine the optimum

temperature range for the ACs production. From the TG/DTG curves, it can be observed that the RM decomposition occurs in three steps with formation of carbonaceous material after 380 °C. The first mass loss step is due to water adsorbed by the material during storage. The second step starting at 228 °C refers to the thermal degradation of the organic material composed of lignocellulose, cellulose, hemicellulose and lignin [21], while the last step is attributed to the thermal decomposition of the carbonaceous material between 380 and 1000 °C.

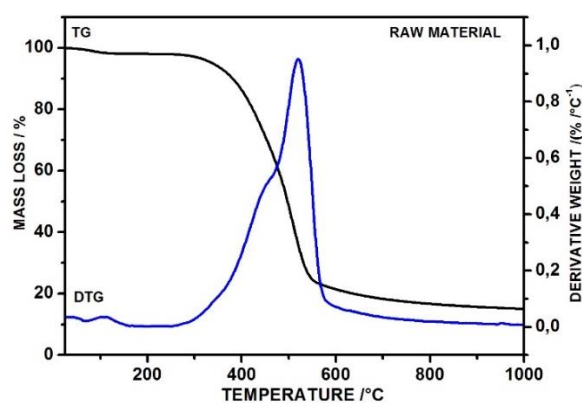


Figure 1. TG–DTG curves of the raw material (RM) under inert N₂ atmosphere (initial mass = 3,52 mg).

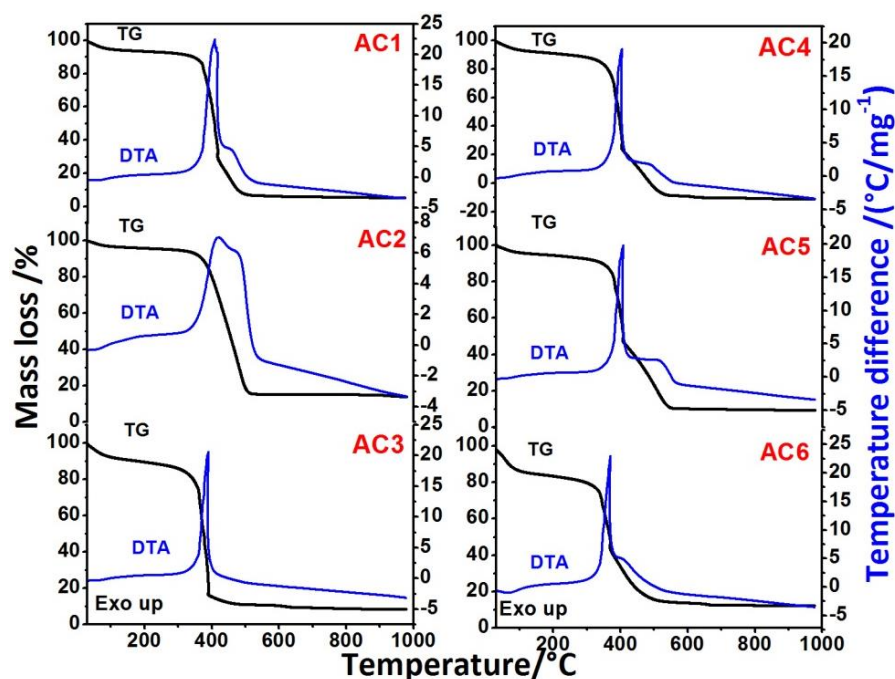


Figure 2. TG–DTA analyses of the activated carbon samples at 500 °C under air atmosphere: AC1 3.58 mg, AC2 2.98 mg and AC3 2.13 mg. Activated carbons at 600 °C: AC4 3.33 mg, AC5 3.19 mg and AC6 3.74 mg.

In summary, the analysis of the RM by TG/DTG, Fig. 1, indicates that the optimum

temperature range for the AC production is above 380 °C, since this region shows a rich carbon content, ideal

for the adsorbent production from the RM studied.

The AC_s were analyzed under air oxidizing atmosphere in order to study their stability and thermal behavior, as well as determine the ash and water contents present in the samples. Thermal analysis TG–DTA for the AC_s at 500 °C in the ratios 1:2:3 of NaOH/RM is shown in Fig. 2 AC1–AC3.

The TG–DTA curves show steps with similar thermal decomposition profiles for all activating agent/RM ratios. The mass losses were accompanied by an endothermic event concerning water adsorbed by the material and two exothermic events related to the oxidation of the carbonaceous material, which led to ash formation, so that 6.0% (AC1), 15.0% (AC2) and 9.0% (AC3). The amount of residue formed can be related to inorganic compounds from raw RM or to the chemical activation process.

The results for the AC_s samples at 600 °C at different activating agent/RM ratios are shown in Fig. 2. Thermal analysis TG–DTA shows that the decomposition occurs basically in three steps. Unlike the AC_s at 500 °C, the thermal decomposition of the AC_s at 600 °C shows similar profile for all samples.

The first mass loss is attributed to adsorbed water, while the others ones are related to intrinsic characteristics of the material like the thermal decomposition of surface groups combined with fragmentation of heteroatom attached to the carbon skeleton and aromatic rings. Such information are corroborated by the thermal decomposition of the carbonaceous material observed, which occurs in two overlapping steps, evidencing the presence of different chemical groups on the surface of the AC_s.

The ash content from the oxidation of the carbonaceous material was 1% (AC4), 11% (AC5) and 12% (AC6). Lastly, the low ash proportions formed for the AC_s at both 500 °C and 600 °C evidence an efficient activation process as well as the removal of the activating agent.

3. 2. Scanning electron microscopy (SEM)

Morphological analysis of the raw material (RM) and of the AC_s (AC1–AC6) performed by SEM, Fig. 3, aimed to visualize the formation of surface pores on the material as well as the morphological characteristics obtained from the activation process at different activating agent /RM proportions, at the temperatures of 500 °C (AC1–AC3) and 600 °C (AC4–

AC6).

In Fig. 3, referring to the RM, the micrographs zoomed in 5.000x show a smooth and irregular surface, while the micrographs of the AC_s at 500 °C and 600 °C, Fig. 4, at the 1:2:3 NaOH/RM ratios show significant morphological changes when compared to the raw RM. After the carbonization process, the structure presented well–developed cavities, intrinsically related to the porosity, which undoubtedly led to the increase of the internal and external surface areas and enhanced the pores availability to adsorb organic and inorganic species [22, 23]. This increase in porosity is effectively elucidated by the BET method.

3. 3. Textural analysis

The textural analysis of the AC_s, shown in Fig. 4 and 6 (AC1–AC6), consisted in determining the surface area by BET method and the pores size distribution by BJH method using nitrogen adsorption-desorption isotherms, respectively. The AC_s adsorption isotherms at 500 °C and 600 °C were followed by the hysteresis phenomenon in all samples, allowing to associate them with the presence of wedge-shaped mesopores, cone or parallel plates according to IUPAC classification.

The hysteresis loops observed in the isotherms, Fig. 4, occurs due to the nitrogen condensation mechanism in the adsorbent pores. This hysteresis phenomenon, which characterizes the existence of a mesoporous structure, can be explained by different saturation pressures during the adsorption process which make the liquid condensates in the pores at relatively higher pressure followed by liquid desorption at relatively lower pressure [21–23].

The development of porosity in the samples can be seen by the increase in the surface area of the AC_s at 500 °C and 600 °C, more evident for the samples produced at higher pyrolysis temperature and at higher activating agent ratios. The results obtained for the surface areas of the AC_s are consistent with the previous statement, since they follow the order AC1 = 309 m²g⁻¹ > AC2 = 479 m²g⁻¹ > AC3 = 889 m²g⁻¹ > AC4 = 557 m²g⁻¹ > AC5 = 902 m²g⁻¹ > AC6 = 1715 m²g⁻¹. Regarding the amount of nitrogen adsorbed by the AC_s, it is observed that the AC6 activated carbon produced at higher pyrolysis temperature and activating agent ratio had the greatest volume of adsorbed gas, which corroborates the surface area data obtained by the BET method.

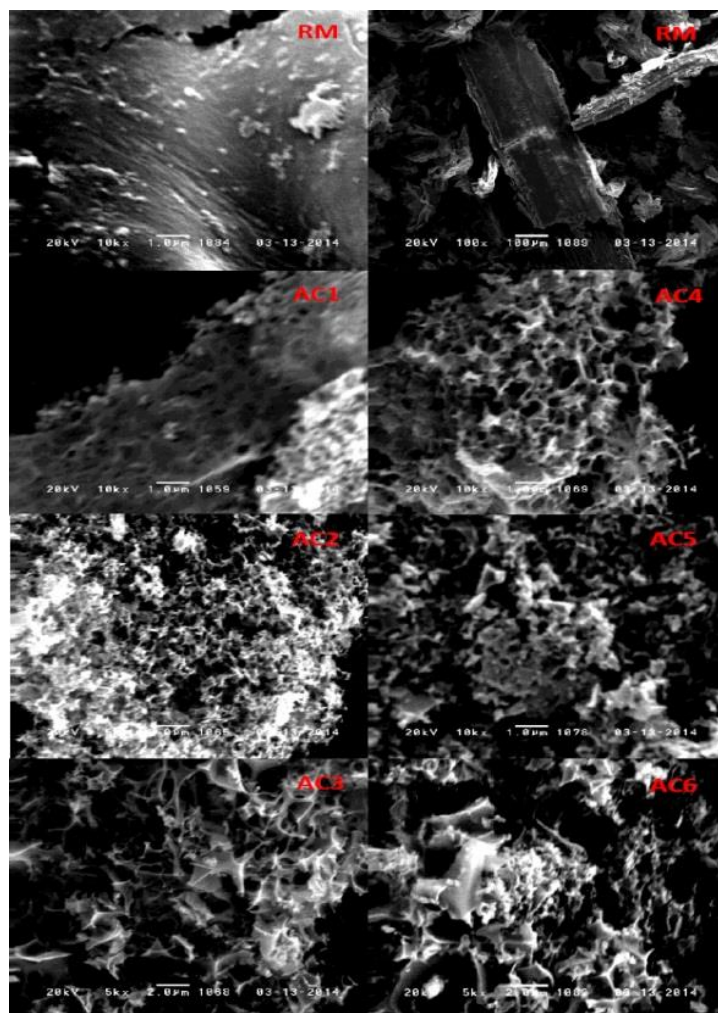


Figure 3. Micrographs obtained by SEM of the raw material (RM) without thermal treatment and of the activated carbons prepared with three activating agent ratios at two different temperatures, 500 °C (AC1–AC3) and 600 °C (AC4–AC6).

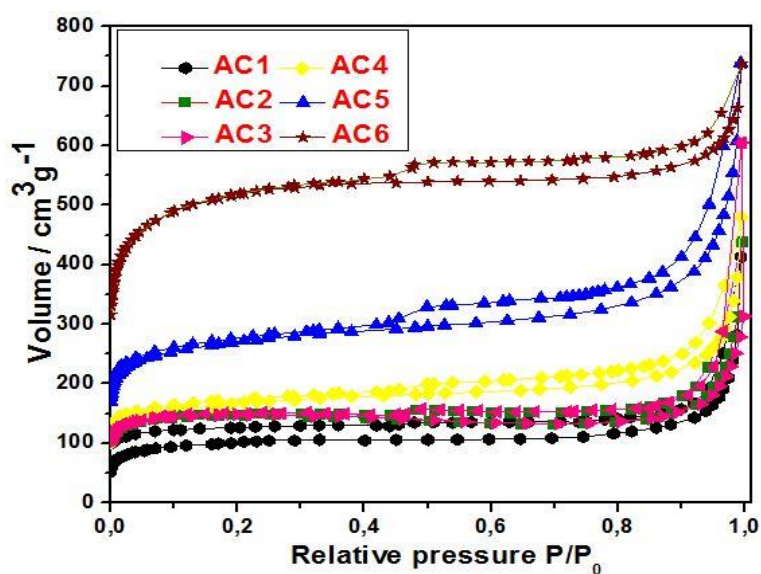


Figure 4. Nitrogen adsorption/desorption isotherms at $-196\text{ }^{\circ}\text{C}$ of the activated carbons prepared with four activating agent ratios at two different temperatures, 500 °C (AC1–AC3) and 600 °C (AC4–AC6).

BJH method was used to analyze the pore diameter of the ACs, Fig. 5. In these curves, it is observed that the highest adsorption occurs within the mesoporous region, between 2 and 50 nm [24]. These findings are consistent with the data observed in Fig. 5.

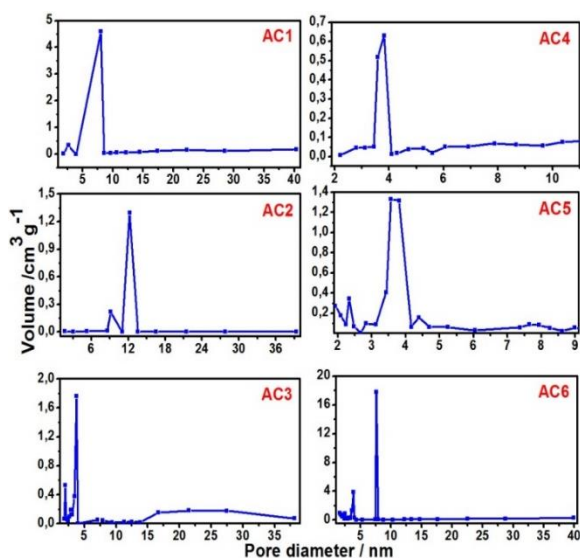


Figure 5. Pore size distribution of the activated carbons prepared with three activating agent ratios at two different temperatures, 500 °C (AC1–AC3) and 600 °C (AC5–AC6) using BJH method for mesoporous material.

3.4. Study of the surface groups by TG/DTG/FT–IR and FT–IR

Surface chemical groups on AC decompose when undergo heating, releasing CO (carbon monoxide) and CO₂ (carbon dioxide) at specific temperatures. Thus, the thermal decomposition of the material with CO₂ release between 100 and 400 °C can be due to carboxylic acids or lactones, while carboxylic anhydrides are products from CO and CO₂ release at the same time in the range of 350 – 620 °C. The surface groups like phenol, ether, carbonyl and quinone release CO only above 700 °C [25].

In the present work, the RM Buriti petiole was modified by thermal and chemical treatments in order to obtain high porosity materials with different surface properties. These materials were characterized by different techniques like TG/DTG/FT–IR in an attempt to identify the surface groups on the ACs produced. The TG/DTG curves of the ACs were divided into five temperature ranges (R1–R5), as shown in Fig. 6. These curves were obtained in N₂ atmosphere and indicate three main mass losses for the samples; the first one between 30 and 200 °C, Fig. 6 (R1) is associated with

the release of physically adsorbed water according to gaseous product monitored by coupled FT–IR technique. The second mass loss step in the range of 200 to around 600 °C (R2–R3) shows only CO₂ in the FT–IR spectra as thermal decomposition product. Above 600 °C (R4–R5) it is observed an increase in CO release and the absence of CO₂ up to 1000 °C.

From these findings on the ACs, it is evident the absence of anhydrides due to the anhydrides decomposition leads to formation of one CO₂ molecule and another one of CO within the determined temperature range of 200 – 600 °C [26]. Thus, in this range surface groups like carboxylic acid and lactone can be present due to release of only CO₂, while between 600 and 1000 °C, release of only CO evidences the existence of groups like quinone, carbonyl and ether on the material surface produced from Buriti petiole.

The RM and the ACs were studied by FT–IR in the solid state in order to corroborate the TG/DTG/FT–IR data. According to the results shown in Fig. 7 and Table 2, it is observed that in the RM spectrum, the broad band in the 3363 cm⁻¹ region can be attributed to the O–H group stretching due to water present in the material while the band in the 2923 cm⁻¹ region can be attributed to C–H stretching. The two bands located at 1602 and 1737 cm⁻¹ may be related to the aromatic C=C stretch or due to the conjugate C=O group. The peak at 1240 cm⁻¹ can be related to C–O bonds of ethers groups, hydroxyls and phenols, which are part of the cellulosic matrix of the RM [27].

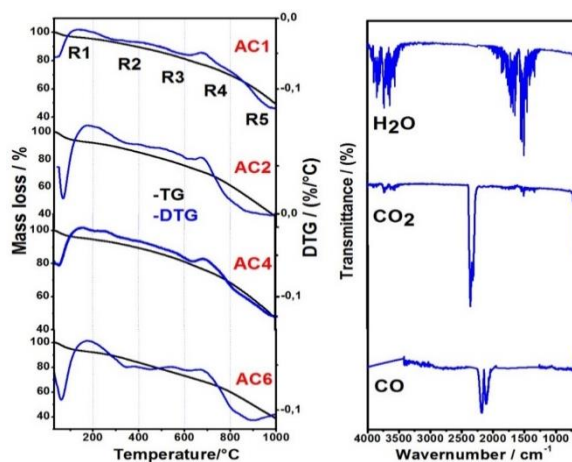


Figure 6. TG/DTG curves and FT–IR spectra of the gaseous products monitored from the thermal decomposition of the activated carbons in N₂ atmosphere.

In the spectra of the ACs samples at 500 °C and

600 °C, changes were observed in the absorption intensities, as well as the absence of bands when compared to the RM spectrum. The occurrence of an intense peak at 1591 cm⁻¹ is indicative of the presence of C=O groups, carbonyl, lactone and quinone conjugated to aromatic rings, while the overlapping bands between 1000 and 1500 cm⁻¹ can be due to the C–O stretching of ethers. These groups represent the basic surface profile after the activation process with NaOH. Thus, the information obtained from the FT–IR spectra showing the existence of C=O and C–O–C groups denote the possibility that the AC samples can

act as basic sites due to the existence of regions rich in π electrons [25–27]. From the TG/DTG/FT–IR and FT–IR data, the main surface groups of the ACs were summarized in Table 2 and the likely chemical structure of the adsorbent material obtained is presented as a model in Fig. 8. On the other hand, the presence of carboxylic and phenolic groups was discarded, since the TG–DTA curves in Fig. 2 and FT–IR spectra in Fig. 7 show a direct relationship between the amount of adsorbed water and the intensity of the band for the O–H group in the 3500 cm⁻¹ region, as seen for the activated carbons AC2 and AC5.

Table 2. Surface groups of the activated carbons prepared with three activating agent ratios at two different temperatures, 500 °C (AC1–AC3) and 600 °C (AC4–AC6).

Surface groups	Literature (cm ⁻¹)	Experimental (cm ⁻¹)	Stretching groups
Carbonhydrogen	2940–2900	2923	ν C–H
Aromaticring	1550–1600	1602–1737	ν C=C
Lactone	1650–1790, 1795	1500–1600	ν C=O
Quinone and carbonyl	1660–1630, 1558	1591	ν C=O
Ether	1000–1300	1100	ν C–O–C

ν = stretching

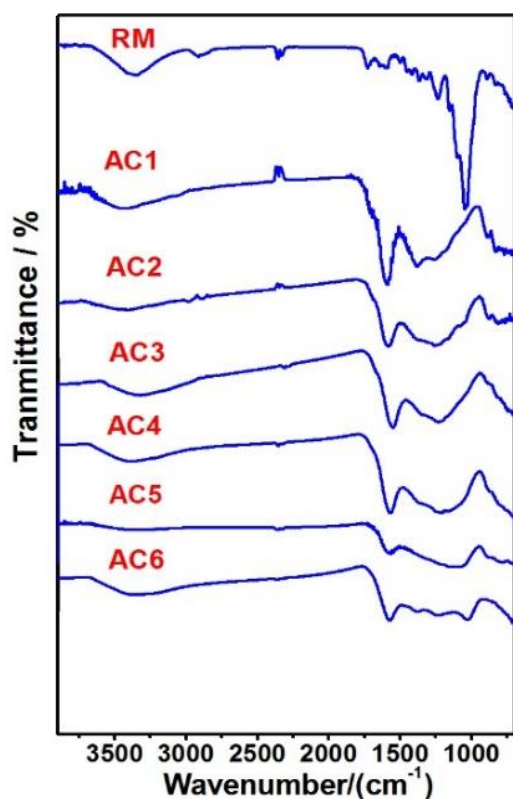


Figure 7. FT–IR spectra of the raw material (RM) and activated carbons prepared with three activating agent ratios at two different temperatures, 500°C (AC1–AC3) and 600°C (AC4–AC6).

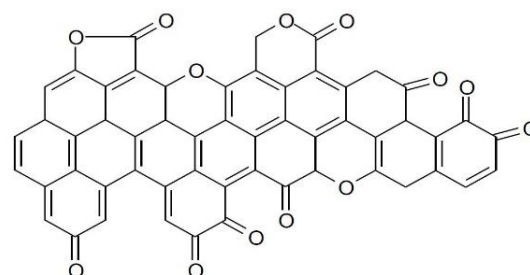


Figure 8. Representative structure of the carbonic matrix and its main surface groups present in the activated carbon samples.

3. 5. Adsorption tests using cationic and anionic dyes

Adsorption tests simulating a water decontamination process were performed in neutral pH to evaluate the adsorption capacity of the ACs obtained for specific application. Using methylene blue and orange G as models of polluting substances, the adsorption capacity of the ACs samples was compared to that one of the commercial activated carbon (CAC).

The results from the adsorption tests with MB and OG dyes show increase of adsorption by AC samples according to the surface area data in Table 3. The difference in the adsorption capacity between OG

and MB is probably due to the molecular size and chemical affinity of surface groups on the AC_s [7, 9, 10]. Furthermore, the presence of anionic groups in the OG molecules probably does not favor the adsorption because the AC_s surface has greater chemical affinity for cationic groups, since the thermal treatment with NaOH activating agent produces basic functional groups on the carbon surface, which enhances the cationic dye adsorption. These affinities are mainly related to interactions among ether, carbonyl, lactone

and quinone groups identified by the FT-IR and TG/DTG/FT-IR techniques.

Therefore, the AC4 sample presented the better cost-benefit relationship to be employed as a filtering agent in effluent treatment plants in industry or for other similar treatments, since its adsorption capacity was near to the other samples at a lower activating agent ratio.

Table 3. Results of the adsorption tests with methylene blue and orange G dyes solutions.

Activated Carbon 500 mg	Concentration Initial of dyes (mgL ⁻¹)	Methylene Blue		Orange G	
		Adsorbed concentration (mgL ⁻¹)	Final concentration (mgL ⁻¹)	Adsorbed concentration (mgL ⁻¹)	Final concentration (mgL ⁻¹)
AC1	100	80.1	19.9	55.7	44.3
AC2	100	89.2	10.8	64.3	35.7
AC3	100	90.0	10.0	84.1	15.9
AC4	100	84.8	15.2	67.6	32.4
AC5	100	95.6	4.40	72.3	27.7
AC6	100	98.1	1.90	88.1	11.9
CAC	100	99.4	0.60	97.9	2.10

CAC = commercial activated carbon

4. CONCLUSION

Drinking water pollution systematically caused by industrial development worldwide is one of the most serious and urgent problems of the modern society to be dealt with. In this context, Brazilian natural resources have a huge potential to be used as alternative and renewable sources of lignocellulosic material for adsorbents production, addressing not only national environmental regulations but also environmental and socio-economic demands. Thus, activated carbons from alternative and renewable biomass source (Buriti petiole) were produced; these adsorbents were obtained with surface area between 340 and 1700 m²g⁻¹ and ash content of about 10%. The pore diameter distribution determined by the BJH method showed formation of mesoporous materials, favorable to adsorption of substances of high molecular weight, like dyes.

Regarding the surface groups of the activated carbons, the samples analyzed by FT-IR and TG/DTG/FT-IR techniques showed formation of basic groups like ether, carbonyl, lactone and quinone, as well as carbonic skeleton associated with double bonds. On the basis of the adsorption tests for Methylene Blue and Orange G dyes, it is possible to affirm that the material studied can be used as

alternative and inexpensive adsorbent. Furthermore, the higher affinity by the cationic dye Orange G is strongly indicative of the presence of basic groups on the material surface, which corroborates the TG/DTG and FT-IR data.

5. ACKNOWLEDGMENTS

The authors thank Ivo Giolito Thermal Analysis Laboratory (LATIG), Professor Massao Ionashiro and Foundations Fundação de Apoio ao Desenvolvimento do Ensino, Ciência e Tecnologia do Estado de Mato Grosso do Sul (FUNDECT), Award Number 0146/12 and Conselho Nacional de Desenvolvimento Científico e Tecnológico (CNPq) for financial support.

6. REFERENCES AND NOTES

- [1] Santhi, T.; Manonmani, S.; Smith, T. *Orbital: Electron. J. Chem.* **2010**, *2*, 101. [\[Link\]](#)
- [2] Darvishi, C. S. R.; Noorimotlagh, Z.; Khatae, A. R.; Shahriy, S.; Nourmoradi, H. *J. Taiwan Inst. Chem. Eng.* **2014**, *45*, 1783.
- [3] Soto, M. L.; Moure, A.; Domínguez, H.; Parajó, J. C. *J. Food. Eng.* **2011**, *105*, 1. [\[CrossRef\]](#)
- [4] Rocha, O. R. S.; Nascimento, G. E.; Campos, N. F.; Silva, V. L.; Duarte, M. M. M. B. *Quim. Nova* **2012**, *35*, 1369. [\[CrossRef\]](#)

- [5] Kunz, A.; Peralta-Zamora, P.; Moraes, S. G.; Durán, N. *Quim. Nova* **2002**, *25*, 78. [\[CrossRef\]](#)
- [6] Guo, Y.; Rockstraw, D. A. *Bioresource Technol.* **2007**, *98*, 1513. [\[CrossRef\]](#)
- [7] Deng, H.; Lu, J.; Li, G.; Zhang, G.; Wang, X. *Chem. Eng. J.* **2011**, *172*, 326. [\[CrossRef\]](#)
- [8] Sud, D.; M., Mahajan, G.; Kaur, M. P. *Bioresource Technol.* **2008**, *99*, 6017. [\[CrossRef\]](#)
- [9] Rafatullah, M.; Sulaiman, O.; Hashim, R.; Ahmad, A. *J. Hazard. Mater.* **2010**, *177*, 70. [\[CrossRef\]](#)
- [10] Bazrafshan, E.; Mostafapour, F. K.; Zazouli, M. A. *African J. Biotechnol.* **2012**, *11*, 1666.
- [11] Yang, K.; Peng, J.; Srinivasakannan, C.; Zhang, L.; Xia, H.; Duan, X. *Bioresource Technol.* **2010**, *101*, 6163. [\[CrossRef\]](#)
- [12] Ramos, P. H.; Guerreiro, M. C.; Resende, E. C.; Gonçalves, M. *Quim. Nova* **2009**, *32*, 1139. [\[CrossRef\]](#)
- [13] Vieira, S. S.; Magriotis, Z. M.; Santos, N. A. V.; Cardoso, M. G.; Saczk, A. A. *Chem. Eng. J.* **2012**, *183*, 152. [\[CrossRef\]](#)
- [14] Juszcak, L.; Fortuna, T.; Wodnicka, K. *J. Food Eng.* **2002**, *54*, 103. [\[CrossRef\]](#)
- [15] Wu, F.C.; Tseng, R.L.; Juang, R. S. *Sep. Purify. Technol.* **2005**, *47*, 10. [\[CrossRef\]](#)
- [16] Gomes, L. R. P.; Lopes, M. T. G.; Bento, J. L. S.; Barros, W. S.; Costa, N. P. G.; Contim, L. A. S. *Crop Breeding Appl. Biotechnol.* **2011**, *11*, 216. [\[CrossRef\]](#)
- [17] Bonesso, S. M. *Instituto Sociedade, População e Natureza* **2011**, *2*, 80.
- [18] Passos, M. A. B.; Mendonca, M. S. *Acta Amaz.* **2006**, *36*, 431. [\[CrossRef\]](#)
- [19] Bansal, R. C.; Goyal, M. *Activated carbon adsorption*. Taylor & Francis: Boca Raton, 2005. [\[CrossRef\]](#)
- [20] Lopez-Ramón, M. V.; Stoeckli, F.; Moreno-Castilla, C.; Marín, F. C. *Carbon* **1999**, *37*, 1215. [\[CrossRef\]](#)
- [21] Naizhen, C.; Darmstadt, H.; Soutric F.; Roy, C. *Carbon* **2002**, *40*, 471. [\[CrossRef\]](#)
- [22] Ioannidou, O.; Zabaniotou, A. *Renew. Sust. Energ. Rev.* **2007**, *11*, 1966. [\[CrossRef\]](#)
- [23] Szymański, G. S.; Karpiński, Z.; Biniak, S.; Świątkowski, A. *Carbon* **2002**, *40*, 2627. [\[CrossRef\]](#)
- [24] Nasrin, R. K.; Campbella, M.; Sandi, Giselle.; Golaś, J. *Carbon* **2000**, *38*, 1905. [\[CrossRef\]](#)
- [25] Rodriguez-Reinoso, F.; Molina-Sabio, M.; Munecas, M. A. *J. Phys. Chem.* **1992**, *96*, 2707. [\[CrossRef\]](#)
- [26] Szymański, G. S.; Karpiński, Z.; Biniak, S.; Świątkowski, A. *Carbon* **2002**, *40*, 2627. [\[CrossRef\]](#)
- [27] Zawadzki, J. *Infrared spectroscopy in surface chemistry of carbons*. In: *Chemistry and Physics of Carbon*. P. A. Thrower (Ed.), vol. 21, Marcel Dekker, New York, **1989**, p. 147-386.